Application Report

SPRA657 - April 2000

Low-Power Real-Time Programmable DSP Development Platform for Digital Hearing Aids

Trudy Stetzler, Neeraj Magotra, Pedro Gelabert, Preethi Kasthuri, Sridevi Bangalore

Digital Signal Processing Solutions

ABSTRACT

This application report describes the development of a new low power binaural wearable digital hearing aid platform based on the TMS320C5000™ fixed point digital signal processor (DSP). This platform is a real-time system capable of processing two input speech channels at a 32 KHz sampling rate for each channel and driving a stereo headphone output. It provides for frequency shaping, noise suppression, multiband amplitude compression, and frequency dependent interaural time delay algorithms. Since the platform is a programmable solution capable of running at 1.8 V for MIPS intensive research and 1 V for actual hearing aid implementation, this platform will enable further research into improving the quality of life for the hearing impaired.

Contents

List of Figures

TMS320C5000 is a trademark of Texas Instruments.

List of Tables

1 Introduction

Approximately 10% of the population suffers from some hearing loss, however only a small percentage of potential wearers actually use a hearing aid. There are several factors affecting market penetration. First, there is the stigma associated with wearing a hearing aid. Second is customer dissatisfaction with the devices not meeting their expectations. Third is the cost associated with the new digital versions of hearing aids [1].

The recent development of commercial hearing aids with digital signal processing capabilities has allowed the development of advanced signal processing techniques to aid the hearing impaired. The result for the wearer of the hearing aid is more accurate sound reproduction with minimum distortion and noise. Almost all of the largest hearing aid manufacturers have digital hearing aid products on the market, and of the 6 million hearing aids sold in 1998, approximately 20% were digital devices [1]. In order to meet the small size and ultra-low power requirements of hearing aids, the existing solutions resort to custom ASIC devices for each hearing aid design. This increases the final cost of the hearing aid to five times the cost of conventional analog hearing aids, which has limited the spread of these digital instruments. By changing to a commercially available programmable DSP approach, the hearing aid companies could significantly reduce their costs, thereby reaching a larger portion of the population with a lower price, better sound quality digital instrument.

One of the major complaints from hearing aid wearers involves the lack of versatility of the devices – they amplify all sounds rather than just those the wearer wants to hear [1]. The existing hardwired devices and proprietary programmable architectures offer only minimal computational performance (MIPs). This lack of a general purpose and fully programmable architecture with sufficient computational capability to implement complex algorithms restricts researchers from advancing significantly beyond the current algorithms to address the wearers complaints. To overcome this limitation, this spplication report describes a new low power real time binaural digital hearing aid platform based on the TMS320C5000 [2] fixed point digital signal processor family. It is a real time system capable of sampling up to two input speech channels at a 32 KHz rate and driving a stereo headphone output. This 1.8 V development platform allows researchers to use the full speed of the TMS320C5000 (currently at 100MIPS) for experimentation and development of sophisticated hearing aid algorithms. These same TMS320C5000 devices can then be used at a reduced power supply voltage of 1V and reduced number of MIPS for the final implementation in the hearing aid. This platform allows researchers to explore new algorithms while providing the portability required for laboratory as well as real world testing and final implementation.

2 Speech Processing Algorithms

Sensorineural hearing loss is characterized by a loss of sensitivity to sounds that varies with signal level and frequency [3]. Speech processing for the hearing impaired can be used to separate the high and low frequencies and improve speech comprehension and listening comfort. This requires a gain adjustment that is both level-dependent (or syllabic compression) as well as multi-frequency dependent [4]. The block diagram in Figure 1 represents the speech processing algorithms implemented on the binaural wearable digital hearing aid platform [5]. The audiologist customizes the hearing for an individual's hearing loss by selecting the appropriate combination of these algorithms to provide the maximum benefit to the hearing impaired person.

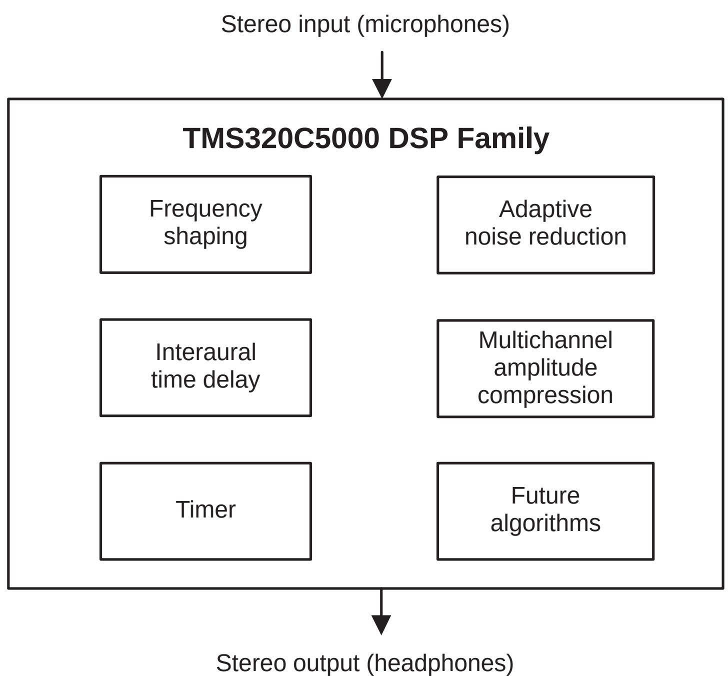

Figure 1. Speech Processing Algorithms for the Binaural Wearable Digital Hearing Aid Platform

The following sections describe the Frequency Shaping, Adaptive Noise Reduction and Multichannel Amplitude Compression algorithms in further detail. These three algorithms are currently considered to be the most critical speech processing algorithms for the hearing impaired. The timer option enables the hearing aid to switch off the drive to the right and left ear pieces, in a mutually exclusive fashion, for a fraction of a second at a time. This option is provided for hearing impaired subjects with severe hearing loss. It is theorized that constant high gain amplification can cause fatigue and the timer option attempts to alleviate this problem without impacting the hearing aid's performance. The interaural delay algorithm permits the therapist to delay the signal going to one ear with respect to the signal going to the other ear on a frequency selective basis. This option is provided based on the theory that if a person has differential hearing loss in the two ears, then in addition to providing compensating gain to the signal going to each ear, there also needs to be some provision for compensating for any internal (within the brain) processing delay between the signals received by the two ears. Both of these algorithms are discussed in further detail in [5].

2.1 Frequency Shaping

The frequency shaping algorithm essentially implements a binaural equalizer using two banks of bandpass filters, one for each ear. This provides for frequency shaping from DC to 16KHz to compensate for a patient's hearing loss. The equalizer uses a variable number (1 to 50, typically 14) of Finite Impulse Response (FIR) filters. Each one of these FIR filters has 50-200 taps, which allows for precision frequency shaping. Linear phase is maintained across the entire frequency bandwidth, and greater than 80dB band isolation is achieved between filters. The therapist/audiologist can interactively (in real-time) choose the number of filters in each bank and select their cutoff frequencies and isolation between different frequency bands. Once the filters have been selected the therapist customizes the spectral magnitude response to the subjects hearing loss by modifying the gain in each individual filter. Figure 2 shows the final result for a subject's left ear. This particular subject had a severe high frequency hearing loss ("ski-slope" loss) and, as indicated in the figure, substantial high frequency gain was provided to compensate for this loss.

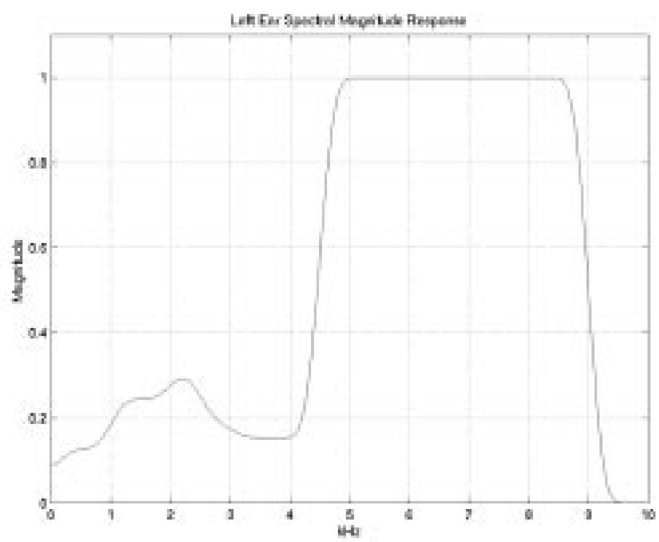

Figure 2. Magnitude Response Designed to Compensate for a Subject's Left Ear Hearing Loss

2.2 Adaptive Noise Reduction

The binaural wearable digital hearing aid platform also incorporates noise suppression as an integral part of the hearing aid. The algorithm works with dual (right and left ear) single input single output channels. First, the input signal is conditioned by a simple one pole highpass pre-emphasis filter to compensate for the low frequency spectral tilt in speech signals [6]. This filter can be placed, at the users option, at one of three locations in the signal flow path as indicated by the boxes labeled 1 through 3 respectively in Figure 3. The core of the adaptive speech enhancement algorithm is the Real-Time Adaptive Correlation Enhancer (RACE) which provides active noise suppression. RACE is essentially an open-loop adaptive FIR filter. Figure 3 shows a basic block diagram of RACE.

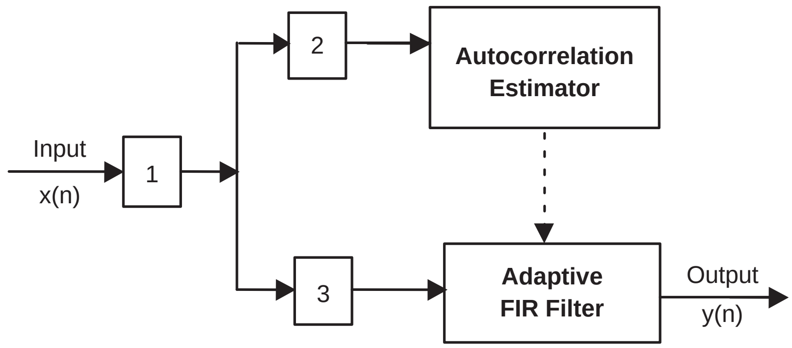

Figure 3. Block Diagram of Real-Time Adaptive Correlation Enhancer (RACE)

RACE estimates values of the autocorrelation of the input using the update equation given by

$$\hat{R}_{xx}(n,k) = \beta\hat{R}_{xx}(n-1,k) + (1-\beta)x(n)x(n+k) \tag{1}$$

where $\hat{R}_{xx}(n,k)$ and $\hat{R}_{xx}(n-1,k)$ are the autocorrelation estimates of the input x(n) at lag value k and at times n and n–1 respectively and β is a smoothing constant whose value lies between 0 and 1. The autocorrelation coefficients are estimated for lag values of k ranging from –L to +L where L is known as the maximum lag. This results in a unique set of (2L+1) autocorrelation coefficients. Typically ‘L’ is chosen to lie between 5 and 7. These values were arrived at by extensive experimentation with hearing impaired subjects. We are currently experimenting with some approaches to modify the correlation function prior to using them as adaptive filter taps. However, our initial approach has been to keep the algorithm simple yet effective. The current approach has proved successful in preliminary human subject testing.

The convergence speed or time constant of RACE can be determined by examining the update equation (1). It represents a first-order difference equation of the form,

$$y(n) = \beta y(n-1) + (1-\beta)x(n) \tag{2}$$

The Z-transform of this equation yields,

$$H(z) = \frac{Y(z)}{X(z)} = \frac{1-\beta}{1-z^{-1}\beta} \tag{3}$$

From the above equation it is seen that the system has one pole at z=β. Hence for the system to be stable the pole must lie inside the unit circle that is, $\beta < 1$.

The impulse response of the system turns out to be a geometric series with a common ratio of β,

$$h(n) = (1-\beta)\beta^{n} \tag{4}$$

If the time constant n_T of the impulse response h(n) is defined as the time it takes for the amplitude to fall to 1/e or 37% of its initial value (1–β), then

$$\frac{1-\beta}{e} = (1-\beta)\beta^{n_T} \tag{5a}$$

or,

$$n_T = -\frac{1}{1n(\beta)} = -\frac{1}{1n(1-(1-\beta))} \tag{5b}$$

This can be approximated as,

$$n_T \approx \frac{1}{1-\beta} \tag{6}$$

Thus it is shown that both stability and rate of convergence are dependent on a single parameter, namely the smoothing constant β. A large value of β implies slow adaptation while a small value of β implies faster adaptation. For example, a β value of 0.987 yields a n_T value of 76, which corresponds to a time of 4msec for a 20 kHz sampling rate. This is less than the short term stationarity of speech which is generally between 5-20 msec. Hence the values of β and L which determine the length of the adaptive FIR filter, should be chosen, so as not to exceed the short term stationarity assumption of speech [7].

The blocks numbered 1 through 3 in Figure 3 indicate the variable location of a pre-emphasis filter, which is essential for most speech enhancement techniques. The energy of a voiced signal decreases approximately at a rate of 6 dB/octave [8]. This is known as the spectral tilt in speech. The first formant in speech is typically in the range of 250-800 Hz and is less important perceptually than the second formant [9]. Hence it is essential to have some form of high pass filtering, known as pre-emphasis filtering to compensate for this spectral tilt. The location of this pre-emphasis filter results in three different RACE configurations as shown in Figure 3 (RACE1, RACE2 and RACE 3). In these acronyms the number corresponds to the location (in the data flow path) of insertion of the pre-emphasis filter.

As mentioned earlier RACE is an open-loop system and one of the main drawbacks is the lack of filter gain control. Hence in order to get a better understanding of RACEs behavior it is useful to study its response when the input x(n*)* consists of a sinusoid in white noise,

$$x(n) = A\cos(\pi\gamma_0 n + \theta) + v(n) \tag{7}$$

where $\nu(n)$ is zero mean white Gaussian noise with a variance equal to σ^2, γ_o is the normalized signal frequency and θ is the random phase. The autocorrelation of the input yields,

$$R_{xx}(k) = \frac{A^2}{2}\cos(\pi\gamma_0 k) + \sigma^2\delta(k) \tag{8}$$

On obtaining its Fourier transform the response of the correlation enhancer, which uses the correlation coefficients as filter taps, comes out to be that of a bandpass filter with center frequency γ_o with a gain of,

$$g = LP(n) \tag{9}$$

where P(n) is the input signal power and L is the maximum lag. Hence a useful gain control procedure is to divide the output by g. An in-depth analysis of the behavior of RACE is given in [10].

Figure 4 shows 300 time samples of a pure sinusoidal wave corrupted with white Gaussian noise with a 0 dB Signal-to-Noise ratio processed through RACE. A 8000 point 1500 Hz, unit amplitude sinusoidal signal and zero mean white noise, both with a variance of 0.5, were generated and added together to get a noisy 0 dB SNR sinusoidal signal. Parameters settings are: Configuration Type = 2, High Pass filter cutoff = 700 Hz, L = 6, β = 0.987, Scaling factor = $1/(L\sigma^2)$.

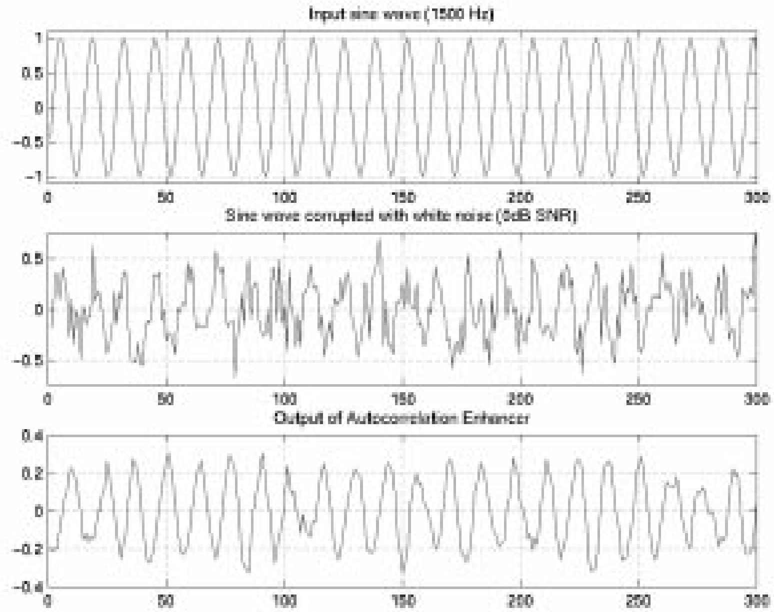

Figure 4. Autocorrelation Enhancement of a Sine Wave Corrupted With White Noise

Figure 5 shows the PDSs corresponding to the time traces shown in Figure 4. It is evident that RACE reduces the amount of background white noise considerably. The noise floor is reduced by approximately 17 dB. To further quantify the performance of RACE by Signal-to-Noise Ratio (SNR) improvement, we define SNR as the ratio of signal variance to noise variance for zero mean data. In the simulation the initial 2000 samples of the waveform consisted of noise alone. For the unprocessed signal and the processed noisy sine signal, the estimated variance over a period where the sinusoidal component was absent, was assumed to be an estimate of noise power ($\sigma^2{}_N$). For each of the files, the variance over a period of signal presence was taken to be a measure of signal plus noise power ($\sigma^2{}_{S+N}$). SNR estimate for each file was then computed as,

$$SNR = 10 \log \frac{(\sigma^2_{S+N} - \sigma^2_N)}{\sigma^2_N} \tag{10}$$

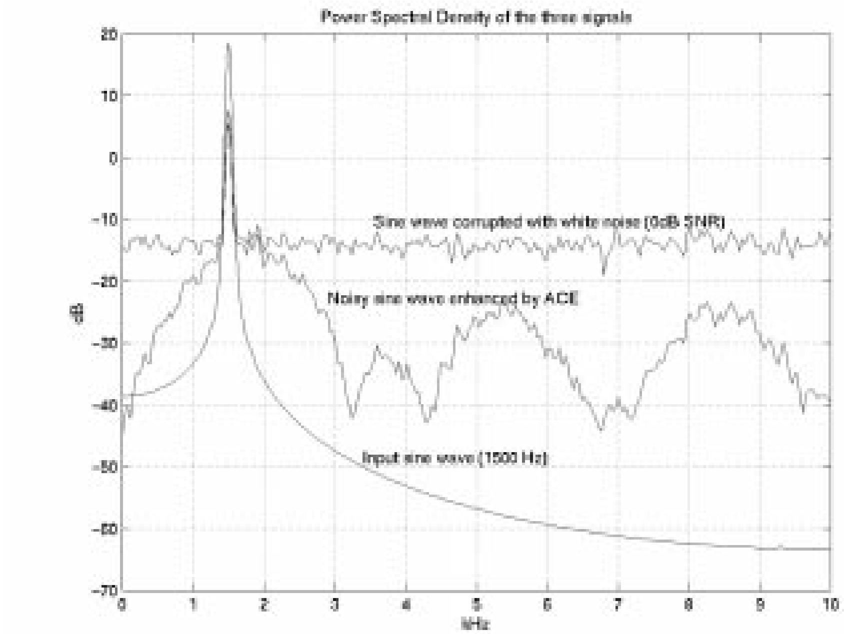

Figure 5. Power Spectral Densities of the Three Signals

SNR improvement for each processing instance was then computed as the difference between output SNR and input SNR,

$$SNR_{improvement} = SNR_{output} - SNR_{input} \tag{11}$$

The SNR improvement for the example shown above came out to be 16 dB.

Figure 6 shows a set of estimated autocorrelation coefficients for the noisy signal along with the corresponding RACE filter magnitude response. As expected, the magnitude response is similar to that of a bandpass filter with a center frequency of 1500 Hz.

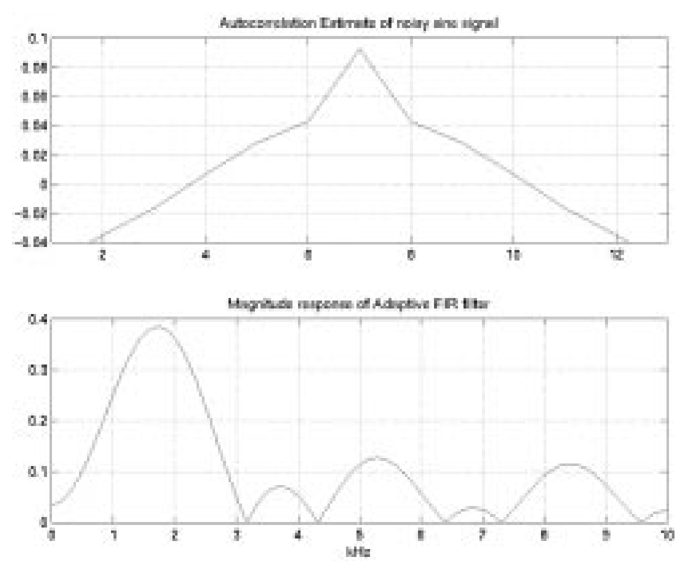

Figure 6. Autocorrelation Estimate of Noisy Sine Signal and Magnitude Response of Adaptive FIR Filter

The effectiveness of RACE in noise reduction applications has also been studied using the CUNY nonsense syllables database and other digitally recorded databases. Figure 7 shows the time traces of the clean nonsense syllable 'za', nonsense syllable 'za' corrupted with cafeteria noise and the output of the autocorrelation correlation enhancer respectively. Processing parameters used were: configuration Type =2, high pass filter cutoff = 700 Hz, L = 6, β = 0.987, scaling factor =1.

The SNR improvement computed for this syllable is 6.4 dB. Even though the output signal trace indicates attenuation over the 'z' part of the syllable the entire 'za' syllable is clearly audible in the output and met with human subject approval in trials. The enhancer output shown in Figure 7 is without applying the gain control suggested in equation (9) to illustrate the artifact that RACE generally provides higher gain for voiced speech. Under normal use conditions, the RACE output is routed through the amplitude compression algorithm to compensate for this attenuation.

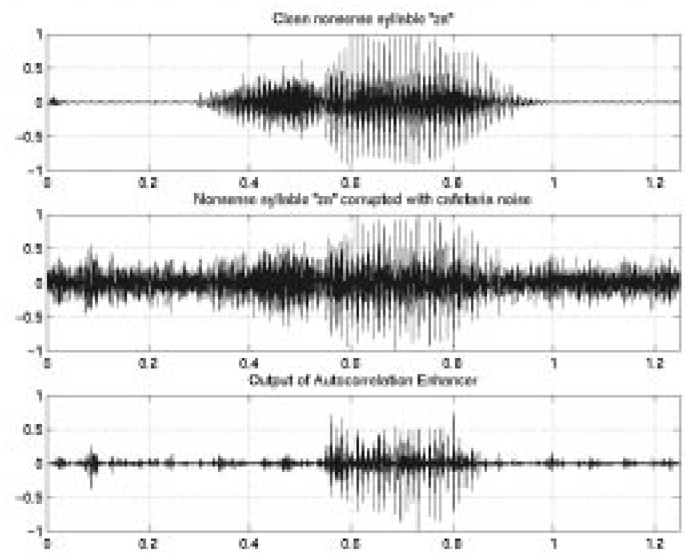

Figure 7. Autocorrelation Enhancement of Nonsense Syllable '*za*'

Some preliminary results (subjective measures) obtained while evaluating the Spectral (frequency) Shaping and RACE algorithms are shown in Table 1 and Table 2. Table 1 summarizes the unaided and aided test scores of some of the test subjects tested at the All India Institute of Medical Sciences (AIIMS), New Delhi, India. (Language: Hindi). Table 2 summarizes the test scores of some of the test subjects tested by administering standard speech discrimination tests in the VA hospital at Truth or Consequence, NM. (Language: English), first using their own aids and then using DIPHA.

Table 1. Test Scores of Subjects Tested at All India Institute of Medical Sciences (AIIMS) (Language: Hindi)

Patient	w/ Own Aid	w/ DIPHA	Age
Patient 1	68%	92%	23
Patient 2	64%	88%	15
Patient 3	56%	72%	75
Patient 4	88%	100%	20
Patient 5	80%	100%	78
Patient 6	40%	64%	50
Patient 7	80%	92%	22
Patient 8	56%	88%	17
Patient 9	8%	36%	28
Patient 10	84%	96%	70
Patient 11	64%	80%	50

Table 2. Test Scores of Subjects Tested at VA Hospital at Truth or Consequences, NM (Language: English)

Patient	w/ Own Aid	w/ DIPHA	Age
Patient 1	54%	100%	74
Patient 2	96%	100%	72
Patient 3	100%	100%	76
Patient 4	79%	94%	63
Patient 5	67%	96%	67
Patient 6	50%	75%	??
Patient 7	75%	92%	76
Patient 8	83%	100%	75
Patient 9	38%	100%	72
Patient 10	13%	63%	87

2.3 Amplitude Compression

In addition to frequency shaping and noise suppression, the platform also permits real time implementation of multiband amplitude compression. Speech amplitude compression is essentially the task of controlling the overall gain of a speech amplification system. It essentially "maps" the dynamic range of the acoustic environment to the restricted dynamic range of the hearing impaired listener.

Amplitude compression is achieved by applying a gain of less than one to a signal whenever its power exceeds a predetermined threshold [12]. Amplitude compression is based on the average power in the signal. The time constant of power estimation is used to modify the attack/release time of the compression algorithm [11]. If x(n) is the discrete time input signal, its estimated power p(n) is given by,

$$p(n) = \beta p(n-1) + (1-\beta)x^2(n) \tag{12}$$

If g is the gain applied to the input x(n) then output y(n) is,

$$y(n) = gx(n) \tag{13}$$

The input and output power are related by,

$$\begin{aligned} p_{out} &= g^2 p_{in} \\ P_{out}dB &= 20\log_{10}(g) + P_{in}dB \\ p_{out}dB &= gdB + P_{in}dB \end{aligned} \tag{14}$$

Figure 8 illustrates a typical linear compression curve. As long as the input power (p_{in}) to the compressor, is less than the input threshold p_{th} no compression takes place and the input is equal to the output. When the input power exceeds the threshold value p_{th}, a gain less than one is applied to the signal. Once amplitude compression is being applied, if the attenuated input power exceeds a specified saturation power p_{sat}, the output power is held at a constant level.

Hence, three regions are considered in the compression scheme based on power estimation. These regions and the corresponding gain applied to the signal in each of these regions, are as listed in equation 15.

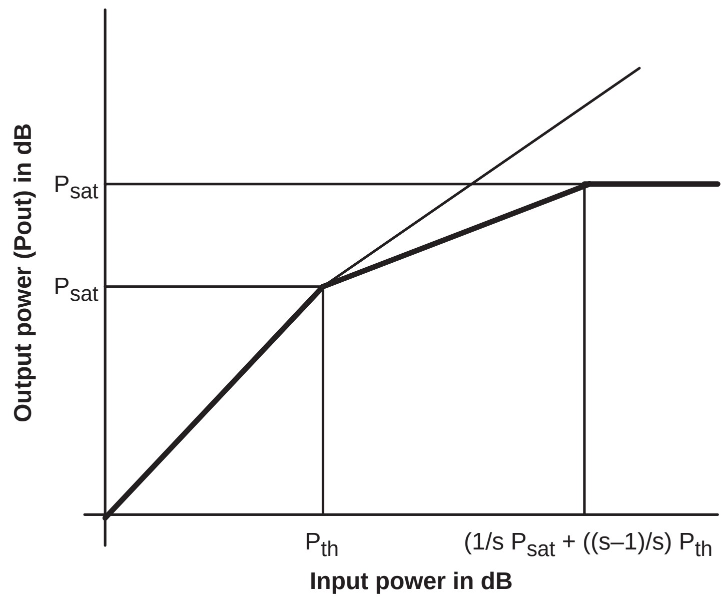

Figure 8. Linear Amplitude Compression

Case 1: $p_{in} < p_{th} \rightarrow$ gain (g) = 1

Case 2: $p_{th} \le p_{in} < \dfrac{p_{sat}^{\frac{1}{s}}}{p_{th}^{\frac{1-s}{s}}} \rightarrow g = \left(\dfrac{p_{in}}{p_{th}}\right)^{\frac{s-1}{2}}$

Case 3: $\dfrac{p_{sat}^{\frac{1}{s}}}{p_{th}^{\frac{1-s}{s}}} \le p_{in} \rightarrow g = \left(\dfrac{p_{in}}{p_{sat}}\right)^{\frac{-1}{2}}$ (15)

In the equations above where *s* is the slope of compression. Note that in real time, p_{in} is not available, so the estimate of p_{in}, p(n) given in equation (12) is used instead.

The simulation data plots shown in Figure 9 demonstrate the efficiency of the compression alogrithm described above. The top trace in Figure 9a corresponds to the nonsense syllable ‘za’. The lower in this figure represents the corresponding compressed output with a lower threshold (p_{th}) of 0.15. Figure 9b illustrates the corresponding power traces. It is evident from the lower (compressed signal) power trace that compression kicks in when the ‘a’ part of the syllable starts. From the corresponding time trace in 9a, note that there is no ‘spiking’ in the time domain – a common artifact in amplitude compressed signals. Typically these spikes are representative of the compression algorithm missing the first few cycles of the loud sound. However, the power estimation employed in our implementation circumvents this problem. An added benefit of this portable prototyping device is that the efficacy of various speech processing strategies, including the algoritms described in this paper, can be measured using test subjects under real world conditions.

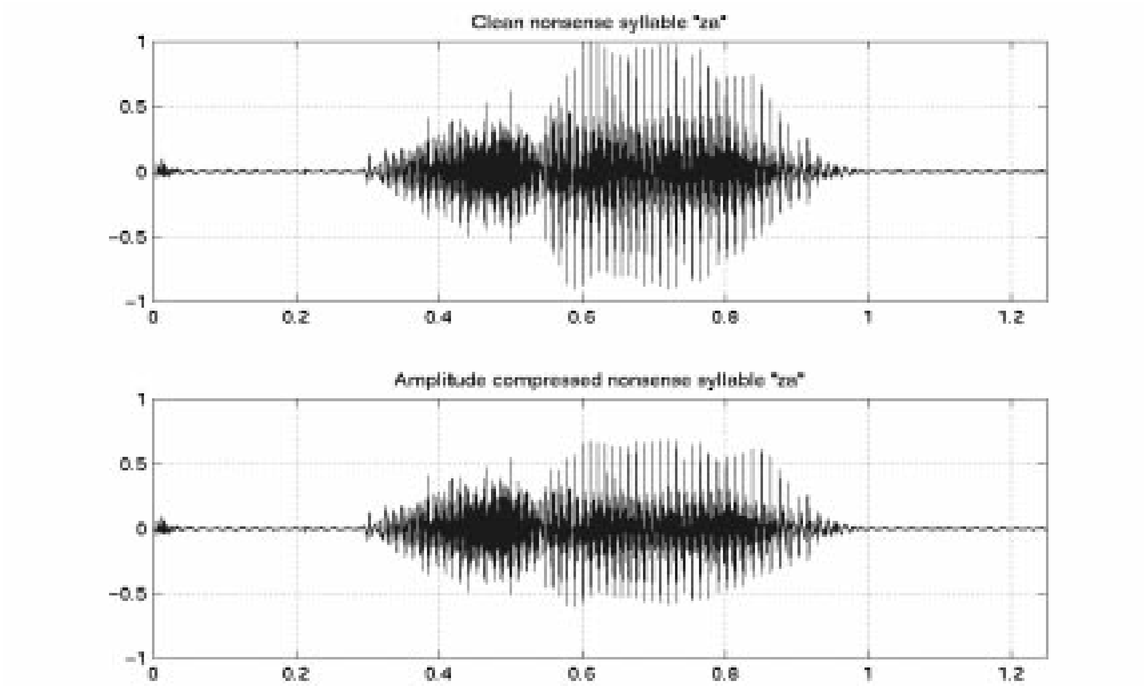

9a. Amplitude Compression and Compressed Output at Lower Threshold

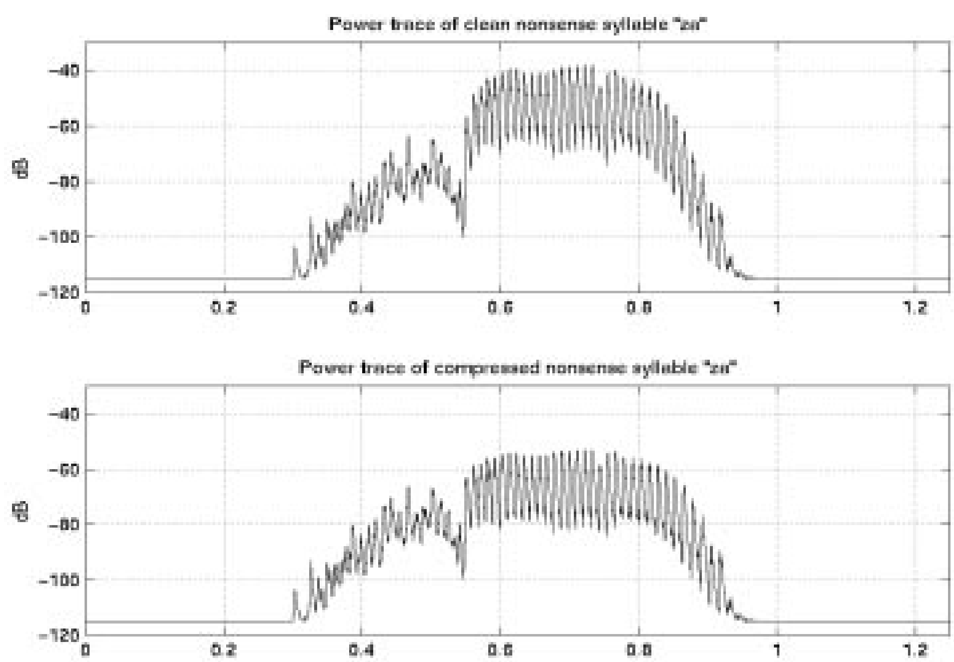

9b. Corresponding Power Traces

Figure 9. Amplitude Compression of Nonsense Syllable ‘za’ – Simulation Data Plots

3 Low Power DSP Platform

3.1 Functional Block Diagram

The functional block diagram for a programmable digital hearing aid is shown in Figure 10.

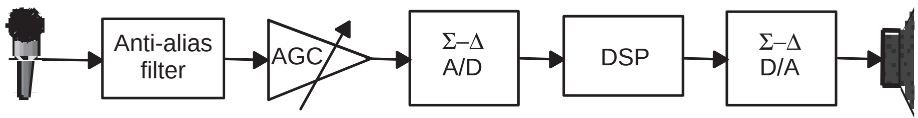

Figure 10. Functional Block Diagram

A low noise microphone converts the incoming sound into an analog signal. This signal is then processed through an anti-alias filer to remove high frequency components. A variable gain amplifier with a compression-limited input stage amplifies the signal prior to the analog-to-digital conversion stage. The analog-to-digital conversion is performed using a 16-bit sigma-delta codec to ensure sufficient dynamic range with a conversion rate of at least 16KHz to ensure adequate sampling of the speech sound components. Ideally, a sampling rate of 32KHz would be preferred in order to provide a quality audio signal to the listener. This platform offers sampling rates up to 48KHz, but at a higher power consumption.

Once the data is converted to the digital domain, the DSP processes the digital stream using the various algorithms described in Section 2 to enhance the speech input. Non-volatile memory is used to store the audio processing algorithms, as well as the parameters for gain control, peak output, and various filter parameters. These parameters are determined through a set of tests performed by an audiologist when the hearing aid is fitted to the user.

The sigma-delta codec converts the processed digital data back to an analog waveform. This waveform is amplified and driven to the speaker. The speaker’s impedance acts as a low-pass filter, removing any high-frequency quantization noise. This entire system must operate from a Zinc-Air battery (1.4V, 60mA-hr), which implies a total current draw on the order of 1-2mA for an operational battery life of 30-60 hours. The end-of-life battery voltage for this battery is approximately 0.9V.

3.2 Low Power Binaural Platform

Figure 11 depicts the low power binaural hearing aid block diagram. This platform was implemented using a TMS320C54x with large on-chip RAM operating at 1.8 V. The TMS320C54x has several power-down modes to minimize power consumption when idle. Unfortunately, the entire system cannot operate at 1.8 V since currently available catalog 16-bit codecs require a 2.7 V supply. Also, to drive the headphones, this implementation requires a stereo headphone amplifier driver that also requires a 2.7 V supply. This amplifier would normally not be present in the final hearing aid implementation.

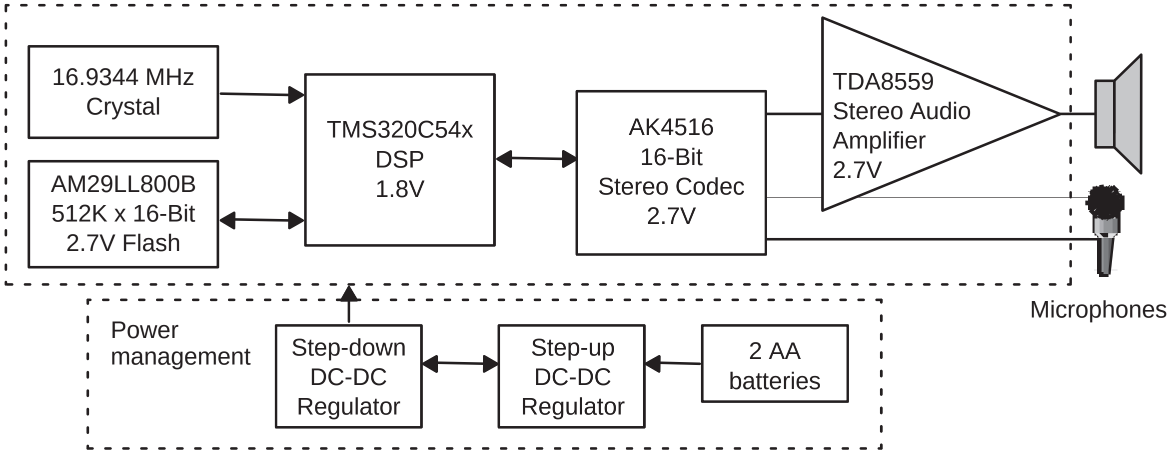

Figure 11. Low Power Binaural Hearing Platform

Figure 12 shows the complete battery powered prototyping system. The system operates at 100 MIPs and 44.1 kHz sampling rate for 23 hours from 2 AA batteries. The prototype dissipates 232 mW, weighs 5 ounces, and is 5.75″x3.69″x1.29″. However, this prototype is designed for maximum flexibility and not minimum size. The system can easily be shrunk to the size of a credit card, using Li-Ion, Li polymer, or Ni-Cd shaped rechargeable batteries as the power source. This prototyping system allows the researcher to explore new algorithms with high levels of computational performance (currently 100 MIPS at 1.8 V) and then use the same programmable DSP architecture with optimized software for operation at 1 V and the reduced MIPs rate of about 20-30MIPs.

Figure 12. Battery Powered Hearing Aid Prototyping System (5.75″x3.69″x1.29″, 5 ounces, 232mW)

For the final hearing aid application, a 1 V voltage regulator is required to maintain a constant power supply independent of battery voltage. A voltage doubler is also required to provide the necessary 1.8V for the codec. Eventually, both the D/A and the voltage doubler could be integrated into the digital signal processor. This approach not only saves space, which is very critical for completely-in-the-ear hearing aids, but also saves power in the final hearing aid implementation. Integrating the D/A into the digital signal processor is achieved by replacing the D/A portion of the codec with a pulse width modulated (PWM) output from the processor. This PWM signal is then amplified with a Class-D amplifier. This is the most power efficient method since Class-AB amplifiers are only ~45-50% efficient compared to the ~80% efficiency of a Class-D amplifier. The speaker impedance is used to demodulate and filter the PWM output, which results in an audio quality signal to the ear [13,14]. Since it is desirable for the hearing aid to fit completely inside the ear, the various components are assembled using known good die. The chips are stacked on top of each other, with the largest device on the bottom, and are connected together via wirebonds. Plastic is then molded around the devices to fit the imprint of a person’s ear canal. In the future, availability of 1V A/Ds would remove the need for a voltage doubler [15,16]. The final hearing aid device would then consist of the DSP, A/D, Flash memory, and Class-D amplifier.

A major issue to address in the final miniaturized hearing aid is acoustic feedback, which can cause the instrument to emit a high-intensity oscillation, known as “whistling”. Aside from being an annoyance to the user, this feedback places sever limitations on the maximum usable gain obtainable from the device. Acoustic feedback occurs when the hearing aid’s receiver produces an acoustic signal that leaks back to the microphone. This feedback usual results from leakage from the ear canal via a vent or from mechanical coupling of receiver motion via the device housing [17]. The cancellation of this feedback involves estimating the feedback signal and subtracting it from the microphone input signal. The most common approach to mitigating feedback in a programmable DSP based solution is to employ adaptive filtering. Since this technique is well documented, we do not address it in the scope of this paper. Several good examples utilizing adaptive filtering to cancel acoustic feedback are found in references [17, 18, 19, 20].

3.3 Power Analysis

Advances in architecture, design, and VLSI technology are producing new generations of digital signal processors with increased computational performance and lower power consumption, enabling these devices to be used in power critical applications such as hearing aids [21]. Figure 13 summarizes the power/performance trend from 1982 through 2000. This trend depicts a halving of the power (mW/MIPs) every 18 months. While the power dissipation is decreasing, it is important to note that the maximum operating rate (MIPs) is either maintained or improved at lower supply voltages.

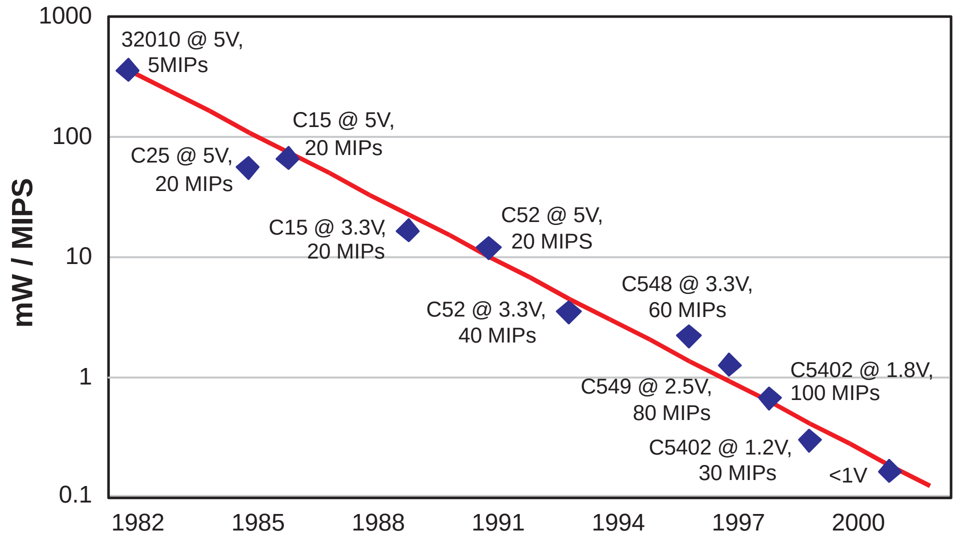

Figure 13. Power Dissipation Trends in DSP

Figure 14 illustrates the performance of the TMS320C5000 as a function of supply voltage. If the technology is constant, then lowering the supply voltage also decrease performance. Therefore, technology scaling and power supply scaling are combined to improve performance while decreasing the total power consumption of the DSP as shown in Figure 14. For example, the 0.15 µm process technology provides 20-30 MIPs performance at 1V while the 0.25µm process provides only 10 MIPs.

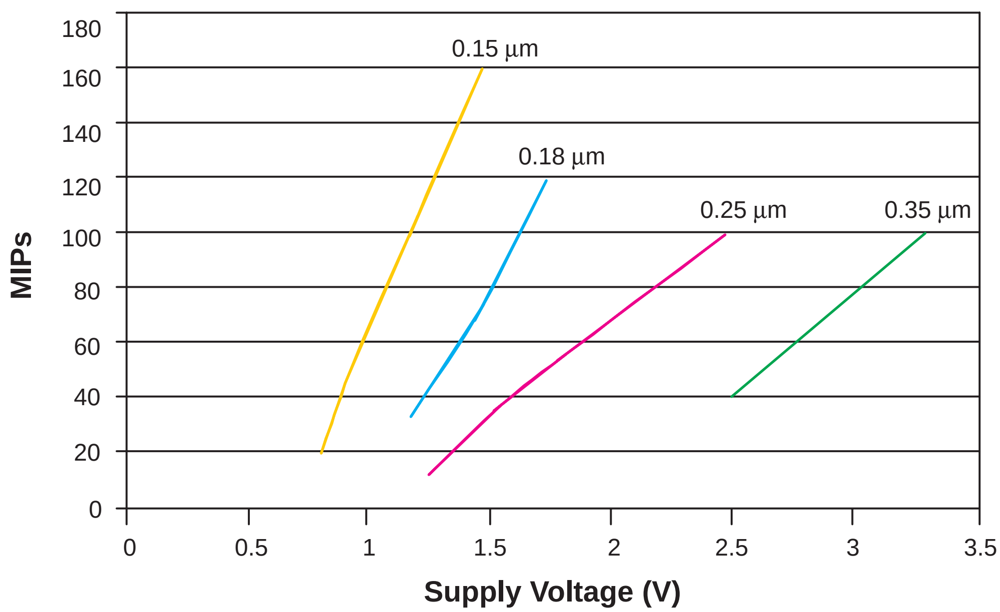

Figure 14. TMS320C5000 MIPs vs. Power Supply

In the last two years, power dissipation has decreased dramatically as shown in Table 3. In 1998, the power consumption was 0.36mW/MIPs at 1.2 V (0.3 mA/MIPs) and the device provided 10 MIPs total processing power. The 1999 version consumes 0.25mA/MIPs at 1.2V (0.3 mW/MIPs) but provides 30 MIPs of total processing power. This same device is available at 1.8 V with 100 MIPs of processing power and 0.37mA/MIPs (0.667 mW/MIPs) power consumption. The TMS320C5000 core being developed for 2000 will consume only 0.18mA/MIPs at 0.9V and will provide 30MIPs processing power (0.162 mW/MIPs), while also providing 160 MIPs maximum performance at 1.5V and 0.3mA/MIPs (0.45 mW/MIPs).

Table 3. TMS320C5000 Power Efficiency

Technology	Voltage (V)	Performance (MIPS)	Power (mA/MIPS)
0.44 µm (1996)	3.3 V	50	0.80
0.35µm (1997)	3.3 V	66	0.60
0.25 µm (1998)	2.5 V	100	0.45
	1.2 V	10	0.30
0.18µm (1999)	1.8 V	100	0.37
	1.2 V	30	0.25
0.15µm (2000)	1.5 V	160	0.30
	0.9 V	30	0.18

4 Conclusion

A new low power binaural wearable digital hearing aid platform based on the Texas Instruments TMS320C5000 fixed point digital signal processor family was developed. The quantization noise issues involved in implementing these algorithms on a fixed-point platform have been described in [22]. The programmability and portability of this system provide a significant improvement over existing hardwired or proprietary solutions for several reasons. First, everyone's hearing loss is different and thus the speech enhancing algorithms need to be tuned to the particular hearing impairment. Second, a person's hearing loss might change with time thus requiring updates in their hearing aid. Third, the speech enhancement algorithms need to adapt to the environment to provide optimum hearing compensation and listening comfort. Fourth, researchers need an open programmable system that allows unbounded performance for algorithm development, yet still provides a low power solution for the final product without modifying the software. Finally, since this solution utilizes a standard catalog part, hearing aid devices can leverage the algorithms already implemented in this architecture to increase the number of features. As these low power programmable devices become available, more sophisticated algorithms and longer battery life will result in an improved quality of life for the hearing impaired.

5 References

1. “World Audiology Products Markets”, Frost & Sullivan, 1997.
2. *TMS320C54x DSP: CPU and Peripherals: Reference Set, Volume #1*, SPRU131; TI web page: http://www.ti.com.
3. E. Villchur, “Signal Processing to Improve Speech Intelligibility in Perceptive Deafness. *Journal of the Acoustical Society of America.* 53: 1646-1657, 1973.
4. B. Edwards, “Signal Processing Techniques for a DSP Hearing Aid”, IEEE International Symposium on Circuits and Systems, June 1998.
5. N. Magotra, Sudheer Sirivara, “Real-Time Digital Speech Processing Strategies for the Hearing Impaired”, International Conference of Acoustics, Speech and Signal Processing,1997.
6. N. Magotra, P. Kasthuri, Y. Yang, R. Whitman, F. Livingston, “Multichannel Adaptive Noise Reduction in Digital Hearing Aids,” IEEE International Symposium on Circuits and Systems, June 1998.
7. Sarala Rajagopalan. Adaptive Correlation Enhancer for Suppression of Background Noise in Speech. M.S thesis, Electrical and Computer Engineering Department, University of New Mexico, May 1995.
8. Ray D. Kent, Charles Reed. *The Acoustic Analysis of Speech.* A.I.T.B.S Publishers, Delhi, India, 1995.
9. J.S.Lim, A.V Oppenheim. “Enhancement and Bandwidth Compression of Noisy Speech”. Proceedings of the IEEE, Vol 67(12), 1586-1604, Dec 1979.
10. N. Magotra. “Seismic Event Detection and Location Using Single Station Three Component Data”. PhD Dissertation, Electrical and Computer Engineering Department, University of New Mexico, October 1986
11. B. Swartz, N. Magotra, “Speech Amplitude Compression”. Proceedings of the IEEE ISE Conference, Albuquerque, NM, 1994.
12. Sudheer Sirivara. “Digital Signal Processing Strategies for the Hearing Impaired”. M.S Thesis, Electrical and Computer Engineering Department, University of New Mexico, July 1997.
13. H. Bresch, M. Streitenberger, Wolfgang Mathis, “About the Demodulation of PWM-Signals with Applications to Audio Amplifiers,” IEEE International Symposium on Circuits and Systems, June 1998.
14. M.C. Killion and G. Village, “Class D Hearing Aid Amplifier,” US Patent No. 4689819; 1987.
15. Y. Matsuya, J. Yamada, “1V Power Supply, 384 kS/s 10b A/D and D/A Converters With Swing-Suppression Noise Shaping”, IEEE International Solid-State Circuits Conference, 1994. Digest of Technical Papers, Page(s): 192 -193.
16. V. Peluso, P. Vancorenland, A.M. Marques, M.S.J. Steyaert, W. Sansen, “A 900-mV Low-Power Δ–Σ A/D Converter With 77-dB Dynamic Range”, IEEE Journal of Solid-State Circuits, Volume: 33 12 , 1887-1897, Dec. 1998.
17. J. A. Maxwell, P.M. Zurek, “Reducing Acoustic Feedback in Hearing Aids”, IEEE Transactions on Speech and Audio Processing, Volume 3, No. 4, July 1995
18. P. Estermann, A. Kaelin, “Feedback Cancellation in Hearing Aids: Results from Using Frequency-Domain Adaptive Filters”, IEEE International Symposium on Circuits and Systems, Volume: 2, Page(s): 257-260, 1994.

19. Y. Park, D. Kim, I. Kim “An Efficient Feedback Cancellation for Multiband Compression Hearing Aids”, Proceedings of the 20th Annual International Conference of the IEEE Engineering in Medicine and Biology Society, Volume 20, No. 5, 1998
20. J. Agnew, “Acoustic Feedback and Other Sudible Srtifacts in Hearing Sids”, Trends in Amplification, Volume 1, No. 2, 1996
21. W. Lee, P. Landman, B. Barton, G. Frantz, “A 1V Programmable DSP for Wireless Applications,” IEEE International Symposium on Circuits and Systems, June 1998.
22. N. Magotra, S. Bangalore, S. Savadatti, P. Kasthuri, S. Divakar, T. Stetzler, P. Gelabert, “Quantization Analysis for Fixed-point Implementation of Speech Processing Algorithms for the Hearing Impaired,” Proceedings of the IEEE Midwest Symposium on Circuits and Systems, August 1999.

IMPORTANT NOTICE

Texas Instruments and its subsidiaries (TI) reserve the right to make changes to their products or to discontinue any product or service without notice, and advise customers to obtain the latest version of relevant information to verify, before placing orders, that information being relied on is current and complete. All products are sold subject to the terms and conditions of sale supplied at the time of order acknowledgment, including those pertaining to warranty, patent infringement, and limitation of liability.

TI warrants performance of its semiconductor products to the specifications applicable at the time of sale in accordance with TI's standard warranty. Testing and other quality control techniques are utilized to the extent TI deems necessary to support this warranty. Specific testing of all parameters of each device is not necessarily performed, except those mandated by government requirements.

Customers are responsible for their applications using TI components.

In order to minimize risks associated with the customer's applications, adequate design and operating safeguards must be provided by the customer to minimize inherent or procedural hazards.

TI assumes no liability for applications assistance or customer product design. TI does not warrant or represent that any license, either express or implied, is granted under any patent right, copyright, mask work right, or other intellectual property right of TI covering or relating to any combination, machine, or process in which such semiconductor products or services might be or are used. TI's publication of information regarding any third party's products or services does not constitute TI's approval, warranty or endorsement thereof.